Assessment of the air change rate of airtight buildings under natural conditions using the tracer gas technique. comparison with numerical modelling

Matthieu Labat, Monika Woloszyn, Géraldine Garnier, Jean-Jacques Roux

Manuscript published in: Building and Environment, Volume 60, February 2013, Pages 37-44
https://doi.org/10.1016/j.buildenv.2012.10.010

Assessment of the air change rate of airtight buildings under natural conditions using the tracer gas technique. Comparison with numerical modelling

Matthieu Labat[1, 2]
Monika Woloszyn[3]
Géraldine Garnier[2]
Jean Jacques Roux[1]

[1]CETHIL, Université de Lyon, CNRS
INSA-Lyon, CETHIL, UMR5008, F-69621, Villeurbanne, France
[2]CSTB - Centre Scientifique et Technique du Bâtiment
24 rue Joseph Fourier, 38400 Saint Martin d'Hères
[3]LOCIE, Polytech Annecy-Chambéry - Campus Scientifique - Savoie Technolac, 73376 Le Bourget-Du-Lac cedex, France

KEYWORDS: air change rate, single-room building, wind and thermal effects, tracer gas measurements, numerical modelling

ABSTRACT:

Under natural conditions, air change rates are very sensitive to specific building elements and to climate conditions, even more so in the case of airtight buildings. Consequently, applying general correlations to such cases may lead to inaccurate predicted air change rates. Still, this approach remains valuable because of its simplicity compared to other methods such as wind tunnelling and CFD simulations. In this paper, the tracer gas concentration decay technique was selected to contribute additional information to classical air-tightness measurements. The measurements were used to fit the coefficients of a general single-node pressure model. Simulation results were found to be consistent with tracer gas measurements most of the time. However, the closeness of the fit is strongly related to the average pressure coefficients from the literature, which were estimated more precisely using the other techniques mentioned above. From a general point of view however, it would seem promising to extend this method to other buildings.

1. Introduction

As saving energy is so important in buildings nowadays, building envelopes need to be increasingly efficient in order to meet current regulation codes. The use of efficient thermal insulation materials has made it possible to reduce energy consumption by reducing heat conduction through the envelope. As this type of heat loss has progressively decreased over the years, the focus has shifted to other heat transfer modes, in particular, convective heat transfers. This type of transfer can be reduced by making the envelope air tight in order to limit air transfers between indoor and outdoor areas. While energy losses are reduced however, other considerations arise such as moisture accumulation and indoor air quality (Blondel and Plaisance 2011, Karlson and Moshfegh 2007). One way to deal with these issues is to improve ventilation systems (Woloszyn *et al.* 2009, Koffi 2009). On the other hand, natural

ventilation is also useful given that it uses no energy at all. Natural ventilation can be easily achieved by considering openings (Santamouris *et al.* 2008) or dedicated building elements such as a solar chimney (Afonso and Oliveira, 2000).

Under natural conditions, air change rates vary greatly because of shifting climates. Indeed, the driving forces are wind and thermal effects, which are both time-dependent. Using constant air change rates would lead to a high level of inaccuracy and detailed approaches are therefore preferable. Numerous studies have been conducted on such cases and have shown that natural driven air change rates are difficult to assess, even when considering simple buildings (Larsen and Heiselberg 2008, Li *et al.* 2001). As a consequence, it would seem difficult to extend the results reported in the literature to existing buildings.

The input of additional information on air transfers would make it possible to select appropriate results from the literature and to enhance modelling. The main objective of this paper is to propose and to test a simple experimental technique which will help improve a classic single-node pressure model. The results from both the measurements and the simulation will be presented and discussed.

This study is based on an existing airtight building with a single opening. The air tightness of existing buildings is commonly measured using depressurizing methods, which provide preliminary information. However, these methods do not provide information on the driving forces of natural ventilation. Wind tunnelling measurements provide useful additional information about wind effect, which is highly dependent on building geometry, envelope permeability and the surroundings (Koinakis 2005). Nevertheless, this method is expensive and time-consuming and in many cases, therefore, other solutions are preferable, such as computational fluid dynamics (CFD) modelling (Van Hoof and Blocken 2010). Still, natural ventilation is time-dependent because it is strictly dependent on climate conditions, which can vary greatly within a single day. Numerous climate conditions should be simulated so that accurate results can be assessed. Another experimental method called the tracer gas technique is described by Cheong (2001). This is an interesting alternative, as it works properly under natural pressure differences. It has already been applied to measure the air change rate in existing buildings by Santamouris *et al.* (2008) and Karlson and Moshfegh (2007).

2. The tracer gas technique

Various tracer gas techniques have been examined. SF_6 is the most commonly used tracer gas as it is detectable at very low concentrations (Afonso and Oliveira 2000, Chao *et al.* 2004, Janssens and Hens 2007, Laporthe *et al.* 2001, Santamouris *et al.* 2008). However, the technique is not limited to a single gas and other gases such as CO_2 (Baker *et al.* 2004, Blondel and Plaisance 2011, Collignan *et al.* 2005) and N_2O (Baker *et al.* 2004, Karlson and Moshfegh 2007, Koinakis 2005, Laporthe *et al.* 2001) have also been found suitable in many cases.

The criteria defined by Cheong (2001) are used to help compare the advantages and drawbacks of these three gases. The results are presented in Table 1 below.

Table 1: Comparison of gases used as tracer gas based on the criteria defined by Cheong (2001)

Criteria	SF_6	N_2O	CO_2
No hazard	Greenhouse effect	< 300 ppm	< 30,000 ppm
No chemical reactivity	✓	✓	✓
Density ($kg.m^{-3}$)	5.11	1.53	1.87
Distinctive from atmospheric gases	✓	✓	no – [300; 600] ppm
Affordable and available	✓	✓	Cheapest solution

Laporthe *et al.* (2001) experimentally compared SF_6 and N_2O in order to investigate the effects of the higher density of SF_6. However, this did not seem to affect the results significantly. In fact, one conclusion drawn was that SF_6 may be preferable because it was more detectable.

Baker *et al.* (2004) experimentally compared N_2O and CO_2, concluding that both were as accurate when experimental solutions were set to limit the drawbacks of using a tracer gas which is already present in the atmosphere. In the end, CO_2 was selected here to obtain the tracer gas measurements as it has less impact on the environment (greenhouse effect) and it is also the least expensive solution.

Concerning the gas injection, several techniques can be found in the literature. Cheong (2001) defines four of them precisely:

- Constant injection: since the flow release rate is known, it is possible to achieve a tracer gas balance so that air-leakage rates are shown. It is a high gas consumption method, but it is well adapted to long-term observations (Afonso and Oliveira 2000).
- Constant concentration: the principle is very similar, but the system is far more complex (Koinakis 2005, Janssens and Hens 2007). When used correctly, such systems can lead to a high level of accuracy. It is also the most expensive of the methods presented here.
- Pulse injection: a small quantity of gas is injected into a duct and its concentration is measured further along (Tanner *et al.* 2000). Consequently, this method is of no interest here.
- Concentration decay: a high quantity of gas is released and mixed into the system. Since the tracer gas concentration is measured along with the decrease, air leakages can be calculated (Blondel and Plaisance 2011).

Concentration decay is the most widespread method used to study the air change rate in a building because it is the easiest to set up and gives accurate results. This method was compared experimentally with the constant concentration method by Chao *et al.* (2004). Both were found to achieve the aim, but the author warned about the importance of achieving a widespread sampling in the building, particularly if the measurements take place in a multizonal building. Similar conclusions were also reached by Van Buggenhout *et al.* (2009). In order to measure the air change rate in our experimental house, it was finally decided to use the concentration decay method.

The air change rate is deduced from the general tracer gas mass balance equation, given in (Cheong 2001) and presented in (1). The calculation of the air change rate will be discussed further in 3.2.

$$V \cdot \frac{dC_{In}(t)}{dt} = S(t) + Q_V(t) \cdot \left(C_{Out}(t) - C_{In}(t)\right) \quad (1)$$

where C_{In} and C_{Out} are the CO_2 concentration of indoor and outdoor air, respectively (ppm), V is the indoor air volume (m^3), Q_V the air leakage rate ($m^3.s^{-1}$) and S is the amount of gas released indoors.

3. Experimental set-up

3.1 A brief description of the experimental set-up

The experimental house is situated in Grenoble, France (latitude: 45.2°E, longitude: 5.77°N) and is exposed to a natural climate. It consists of a single-room building, the dimensions of which are designed to be representative of a living room (4.56×4.55×2.36 m^3 interior dimensions). The indoor air volume is approximately equal to 49 m^3 (this value will be used further to compute the air change rate of the whole test house, as presented in (1)).

The structure is made of spruce studs (section: 0.07×0.165 m^2), positioned every 0.60 m. The walls are composed of gypsum board on the indoor side, cellulose wadding used as an insulation material between the spruce studs, particle board on the exterior side, a rain screen, a ventilated air gap and wooden cladding. The ceiling and the floor are heavily insulated and vapour transfer is prevented by two layers of vapour barrier. Further details about the test house can be found in Piot *et al.* (2011).

The roof is a typical tiled French roof with two 30° slopes facing north and south. The floor has been elevated to 0.57 m above the ground in order to simplify the boundary conditions for the numerical models. The door is located in the middle of the northern face and has been insulated with polystyrene in order to achieve a homogeneous level of insulation.

The test house is also equipped with a ventilation system that is located in the attic: the indoor opening is located in the ceiling while the outdoor opening is located close to the eaves on the western face, 3.43 m up the wall of the experimental house, as shown in Fig. 1(a and b). Another opening is located on the door but has been sealed to increase the air tightness of the building. The indoor temperature and relative humidity are also measured, and a weather station, located close to the test house, records the climatic conditions every 10 min. In particular, wind speed and direction are measured 8 m above the ground.

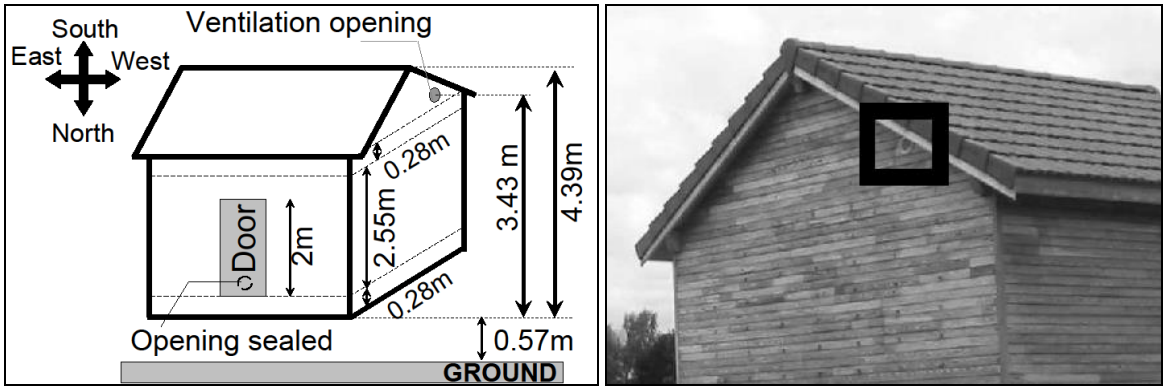

Fig. 1: Scheme of the experimental house with the door on the northern side and ventilation opening on the western side (a) and picture of the ventilation opening (b)

3.2 Tracer gas equipment and setting the initial and final indoor concentrations

The outdoor CO_2 concentration varies throughout the day, even though the experimental house is not set too close to any human activity area. In order to monitor this, a first gas analyser was set up outside at the weather station. Preliminary measurements showed that the outdoor CO_2 concentration remained between 400 and 600 ppm for several months, as shown in Fig. 2. A second analyser was set indoors, while the outdoor CO_2 concentration remained monitored.

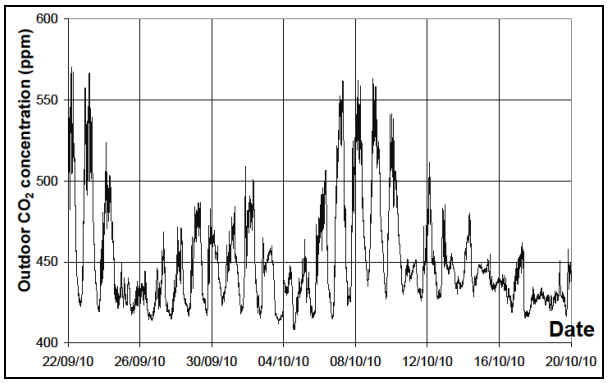

Fig. 2: Outdoor carbon dioxide concentration measured from 22/09/2010 to 20/10/2010

Both devices measure the infrared absorption of gases and are calibrated to detect CO_2. The indoor analyser is equipped with a pump which continuously samples indoor air. To enhance the sampling efficiency, four ventilators were installed to mix indoor air and four sampling tubes were added to the analyser. Carbon dioxide is released from a bottle set inside the experimental house.

In order to minimize the uncertainty related to the outdoor CO_2 concentration, the indoor concentration should be set far higher than the outdoor concentration. At the same time, it is better to reach the gas analyser's saturation rate in order to take advantage of its sensitivity. These two limits are used to define the initial and final indoor concentration, respectively $C_{In}(t=0)$ and $C_{In}(t=t_{Stop})$. To first order, they can be used as boundary conditions to solve (1), considering the average outdoor concentration $\overline{C_{Out}}$, a constant air change rate and no gas release. As a consequence, the elapsed time $t_{Elapsed}$ while the indoor concentration decreased from $C_{In}(t=0)$ to $C_{In}(t=t_{Stop})$ depends on these two limits, as presented in (2).

$$t_{Elapsed} = \frac{V}{Q_V} \cdot \ln\left(\frac{C_{In}(t=0) - \overline{C_{Out}}}{C_{In}(t=t_{Stop}) - \overline{C_{Out}}} \right) \quad (2)$$

It is preferable to conduct a single experiment over several hours so that the outdoor conditions variations have a detectable influence and are easier to identify. Based on preliminary experiments, the average air change rate and outdoor CO_2 concentrations were estimated equal to 6 $m^3.h^{-1}$ and 500 ppm, respectively. The indoor gas analyser range is [0; 10,000 ppm]. The initial concentration was set at 9,500 ppm (this value is preferred to 10,000 ppm to avoid extreme scale values). The final CO_2 concentration was set at 2,000 ppm, so the indoor concentration is at least four times higher than outside. As a consequence, the average elapsed time for a single experiment should reach 15 h.

Similarly, the average air change rate can be deduced from (2), measuring the elapsed time only. This is a very convenient way to discuss the general influence of outdoor conditions, yet a detailed analysis would still contribute more information. This approach will be discussed further in 5.1.

Before carrying out air change rate measurements, several preliminary tests were conducted and aimed at checking:

- The efficiency of the sampling system (ventilators and sampling tubes);
- The low impact of indoor air mixing on the global air change rate;

- A good match with estimated extracted rates when the ventilation system was active (three air changes per hour);
- Low reactivity between carbon dioxide and indoor sides and with water vapour.

4. Air change rate modelling

4.1 General equations

Air can move into and out of the building by several means: through openings (here, the ventilation opening located on the western face), through walls because of their air permeability (here, the four vertical walls) and through cracks or at junctures (here, at the door frame).

Once the N air paths have been identified, it is necessary to consider the pressure field all around the building and to compute a pressure balance in order to correctly model air transfers throughout the whole building (Koffi 2009). For each single i air path (with i from 1 to N), both wind and thermal effects have to be estimated. Next, the pressure difference between indoor and outdoor air dP_i (Pa) can be evaluated using (3). As wind and thermal effects vary quickly within a day, each pressure value is assumed to be time-dependent.

$$dP_i(t) + P_{Int}(t) = P_{Dyn,i}(t) + dP_{Th,i}(t) \quad (3)$$

where P_{Int} is the indoor air pressure (Pa), P_{Dyn} is the dynamic pressure induced by wind (Pa) and dP_{Th} is the pressure difference induced by the thermal effect (Pa).

Next, related airflow rates can be estimated using the general relationship (4).

$$Q_{V,i} = C_i \cdot \left(dP_i(t)\right)^{n_i} \quad (4)$$

where $Q_{V,i}$ is the air flow ($m^3.h^{-1}$), C is the discharge coefficient ($m^3.s^{-1}.Pa^{-n}$), n is a non-dimensional coefficient which characterizes the flow (1 is for laminar flows, 0.5 for turbulent flows). Every value is related to the i air path being considered.

Finally, the N airflows are used to compute a mass balance which leads to the calculation of the indoor pressure P_{Int} used in (3). To avoid numerical problems, (3) is first computed using the indoor pressure from the previous time step.

As already mentioned, wind tunnel measurements would provide accurate and useful information, but these take too long to set up. General results from the literature have therefore been used to describe the wind effect. This can be estimated very simply by computing the dynamic wind pressure as presented in (5):

$$P_{Dyn,i}(t) = \frac{1}{2} \cdot \rho_{Out}(t) \cdot C_{P,i}(\theta) \cdot V_Z(t,z)^2 \quad (5)$$

where ρ_{Out} is the density of outdoor air ($kg.m^{-3}$), C_P is a non-dimensional coefficient depending on wind incidence (θ) and V_Z ($m.s^{-1}$) is the wind speed at wall altitude z (m) away from the test house.

In order to evaluate the pressure difference induced by thermal effects (the so-called stack effect), the general relationship (6) was used. This requires the definition of a single parameter; the altitude z_i (m) of the openings and leakages through which air can move.

$$dP_{Th,i}(t) = -g \cdot z_i \cdot \left(\rho_{Out}(t) - \rho_{In}(t)\right) \quad (6)$$

where g is gravity (= 9.81 $m.s^{-2}$)

4.2 Using air tightness measurements to estimate air flow rates

Air tightness tests (referred to below) rely on creating significant pressure gradients between indoor and outdoor climates. Here, this has been achieved using a device called a Permeascope®, developed by the French company ALDES. This device was selected over the well-known Blowerdoor® technique because its design is much better suited to small airtight rooms. Indoor air is extracted by means of the ventilation duct (see Fig. 3(a)) and the extracted air flow rate is measured. Even if these kinds of tests take place under greater pressure differences (from 20 to 100 Pa) than those occurring under natural conditions (from 2 to 20), Walker *et al.* (1998) have shown that (4) is still valid.

As pressure and air flow rates are both measured, C_i and n_i values such as the ones used in (4) can be estimated by performing linear regressions on the measurements. This is not immediate however, because a single test includes the air flows coming from several air paths (here, from the four vertical walls and from the leakages at the door frame).

A vapour barrier is another material commonly used in wood-framed houses to prevent moisture damage, which also strongly reduces air transfers and contributes to achieving airtight buildings. Here, a vapour barrier which has an impact on moisture transfers equivalent to that of an 18-m-thick air layer (Sd = 18 m), was placed in the vertical walls. A second air tightness test was carried out and the results are presented in Table 2. To allow quick comparison, the I_4 value (from the French standard) was included. This is the ratio of the air change rate occurring under 4 Pa to the building surface (21 m^2). Indeed, 4 Pa is roughly representative of pressure differences occurring under natural conditions.

Table 2: Air tightness measurements obtained with and without the vapour barrier

Test type	Vapour barrier	C ($m^3.s^{-1}.Pa^{-n}$)	n (-)	I_4 ($m^3.h^{-1}.m^{-2}$)
Air tightness	No	5.64	0.69	0.62
Air tightness	Yes	2.92	0.73	0.27

Even if lower I_4 values can now be achieved with passive buildings, the envelope air tightness level is high compared to most existing buildings, as presented in Sfakianaki *et al.* (2008). When assuming that the leakages at the walls are reduced to almost naught when the vapour barrier is in place, it becomes apparent that half the leakages are located at the door frame. A similar conclusion was also reached by Piot (2009) considering other measurements. When assuming that the remaining leakages (the second half) are equally distributed over the four vertical walls, (4) can be rewritten for the door as (7a) and for a single vertical wall as (7b) (the pressure difference is bound to be different for every single vertical wall).

$$Q_{V,Door}(t) = \frac{C}{2} \cdot \left(dP_{Door}(t)\right)^n \quad (7a)$$

$$Q_{V,Wall}(t) = \frac{C}{8} \cdot \left(dP_{Wall}(t)\right)^n \quad (7b)$$

The air flow rate which occurs through the ventilation opening remains to be defined. A third test (see Fig. 3(b) referred to later as the global airflow was therefore carried out, during which the air was extracted through the opening located at the door (the seal was removed for this test only). Leakages at the door frame and through the walls were also taken into account, as shown in Fig. 3(a). The results are presented in Table 3.

Table 3: Comparison of the air tightness measurements with the global airflow measurement

Test type	Vapour barrier	C ($m^3.s^{-1}.Pa^{-n}$)	n (-)	I_4 ($m^3.h^{-1}.m^{-2}$)
Air tightness	Yes	2.92	0.73	0.38
Global airflow	Yes	13.03	0.60	1.43

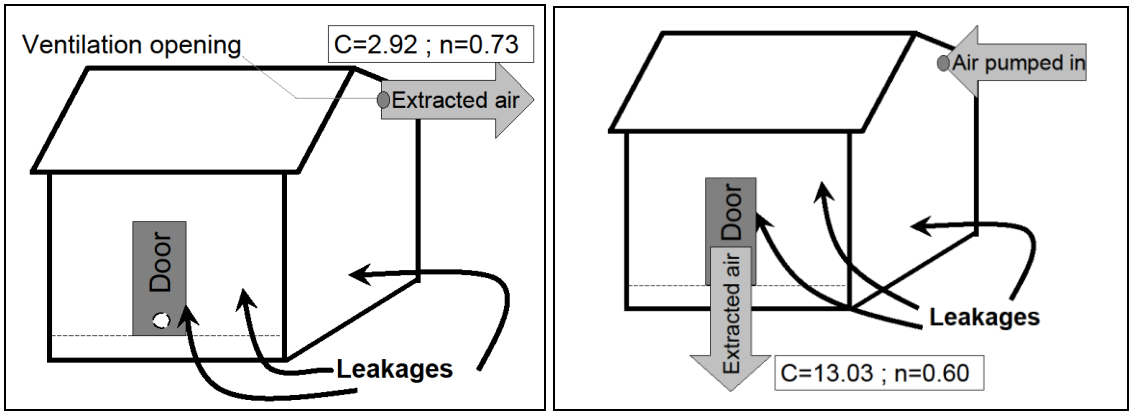

Fig. 3: Scheme of the air tightness test principle (a) and the global airflow test principle (b)

When assuming that the leakages at the wall and the door frame are the same in both experiments, the airflow rate crossing the ventilation opening can be deduced by subtracting the air tightness measurements from the global airflow measurements. So (4) can be rewritten as (8) in order to model the air flow through the ventilation opening.

$$Q_{V,Opening}(t) = 13.03 \cdot dP_{Opening}(t)^{0.60} - 2.92 \cdot dP_{Opening}(t)^{0.73} \quad (8)$$

4.3 Uncertainties on wind and thermal effects

Modelling wind and thermal effects may be difficult to achieve for a real building. Firstly, the thermal effect can be easily computed at the ventilation opening given that its height $h_{opening}$ is clearly identified. This is not the case when evaluating the thermal effect for leakages spread over the entire height of the wall, as illustrated in Fig. 4(a).

Secondly, the pressure field all around the building is non-homogeneous and depends on wind direction: this is mathematically represented by the use of the C_P values in (5). However, these values are also strongly dependent on the building geometry, as shown by Uematsu and Isyumov (1999). The dependency is greatest when looking at specific locations, such as the roof and its edges. Unfortunately, this is where the ventilation opening is located. Moreover, the wind effect is very significant on an opening, which results in higher uncertainties on the airflow rate modelled at the ventilation opening, as illustrated in Fig. 4(b). At the same time, the vertical walls are covered with an open jointed cladding, which may also affect the pressure field acting on air transfers.

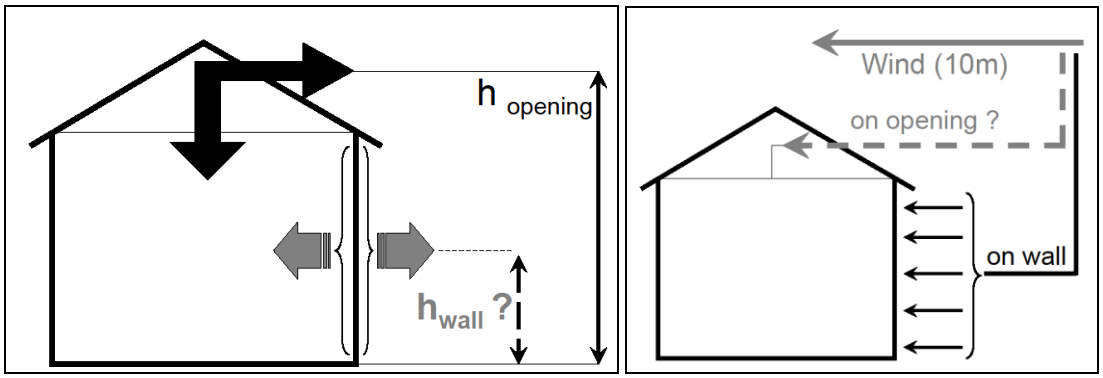

Fig. 4: Difficulties assessing the thermal effect on a widespread area (a) and wind effect at a specific location (b)

An alternative way of modelling thermal effects is to set two equivalent heights h_{Wall} and h_{Door} which would represent the global thermal effect at the walls and at the door, respectively. Concerning the wind effect, it was decided to use general C_P values (see Table 4), which were already proposed in the HAM-Tools model for vertical walls.

Table 4: C_P values depending on the wind incidence θ on the walls according to (Sharag-Eldin 2007)

θ (°)	0	15	30	45	60	75	90	105	120	135	150	165	180
C_P (-)	0.77	0.69	0.54	0.35	0.08	−0.23	-0.61	−0.88	−0.92	−0.77	−0.58	−0.50	−0.42

It is well known that pressure coefficients vary greatly with the building geometry, as presented in Uematsu and Isyumov (1999) and Larsen and Heiselberg (2008). (Costolla *et al.* 2010) advise conducting detailed studies to assess these pressure coefficients accurately, even when the building geometry studied is simple, as here. Indeed, the authors showed that using average pressure coefficient values can lead to substantial errors. Moreover, errors were found to be the greatest when the openings were the smallest; the ratio exceeded 5 in their study. However, the authors also indicated that few methods are able to achieve this goal (wind tunnel experiments and detailed CFD studies, for example). Most of the time, these means are both expensive and time-consuming. As a consequence, the results reported in the literature could still be used and should fit with average trends.

Local wind speed in (5) is simply estimated, as presented in Hagentoft (2001): it is based on formula (9), which considers a logarithmic wind speed profile. It requires the use of a wind speed measurement V_{10} obtained 10 m above the ground. In order to model the influence of the surroundings, two constants are introduced and called “terrain coefficients” (k; a). The values given by the author are reported in Table 5.

$$V_Z = V_{10} \cdot k \cdot z^a \tag{9}$$

Table 5: Terrain coefficients used in (4) (Hagentoft 2001)

Terrain coefficient	k	a
Open flat country	0.68	0.17
Country with scattered wind breaks	0.52	0.20
Urban	0.35	0.25
City	0.21	0.33

Little computational work is needed to find the coefficient combination which would best represent the air transfers. It comprises equivalent heights {h_{Wall}; h_{Door}} and terrain coefficients {k; a}.

5. Results and discussion

5.1 Tracer gas measurements and general analysis

Twelve experiments, conducted from October 2010 to January 2011, are listed in Table 6. The last two columns indicate average values so as to compare experiments, yet further calculations use time-dependent values. The average airflow rate (Qv) calculation is based on (2) and uses the elapsed time measured.The very last column indicates the temperature difference between indoors and outdoors, representative of the thermal effect. The moisture content difference is also influential and will be taken into account in further calculations. In all cases the electric heater was active and maintained indoor air at a constant temperature. Finally, two distinct regimes were observed during experiment no. 1, separated 3 hours 15 minutes after the beginning of the experiment, so results were split in two lines in Table 6. Results for this specific case will be discussed further.

Table 6: Tracer gas measurements from October 2010 to January 2011, elapsed time while the indoor concentration decreased from 9,500 ppm to 2,000 ppm and average weather conditions

no.	Date	Elapsed time (h)	Average airflow rate ($m^3.h^{-1}$)	Average wind speed ($m.s^{-1}$)	Average temp. difference (°C)
1a	04/10/2010	3h15 (1)	8.4	6.6	2.9
1b		24h04 (2)	2.6	1.2	7.4
2	06/10/2010	30h22	3.0	1.0	7.5
3	08/10/2010	26h39	3.4	1.3	10.5
4	11/10/2010	26h25	3.4	1.2	10.8
5	12/10/2010	17h52	5.0	1.3	18.3
6	15/10/2010	17h13	5.2	1.5	21.2
7	03/01/2011	14h59	6.0	2.2	28.2
8	04/01/2011	15h54	5.6	1.7	26.4
9	06/01/2011	13h48 (3)	4.6	2.9	19.8
10	07/01/2011	4h58	18.0	5.1	10.5
11	10/01/2011	19h14	4.7	1.6	21.5
12	25/01/2011	13h39	6.6	1.8	27.4

(1) Based on the indoor CO_2 decrease from 9,500 to 5,720 ppm
(2) Based on the indoor CO_2 decrease from 5720 to 2,000 ppm
(3) This experiment was stopped when the indoor CO_2 concentration reached 3,100 ppm

The results clearly show that the elapsed time can be very different from one experiment to another: it is more than 30 h long for experiment no. 2 and can diminish to almost 5 h for experiment no. 10. As the average airflow rate is computed directly from the decay of the carbon dioxide concentration, it closely follows elapsed time values and varies from 3 to 18 $m^3.h^{-1}$ (average air change rates ranging from 0.06 to 0.37 h^{-1}). Given the rather low indoor air volume and low air permeability of the test house to air, results will be discussed further by considering the average airflow rather than the air change rate.

It should be noted that considering average weather conditions may lead to poor interpretation. Indeed, the temperature difference can strongly vary during a single experiment. For example, it increased from almost 0 to 15°C during experiment no. 2 (see Fig. 5(b)). This results in an increase of the air change rate, accelerating the CO_2 concentration decrease, as it can be seen in Fig. 5(a). When the temperature difference remains the same and under low wind speed conditions, the air change rate

does not vary much (see experiments no. 6 and no. 8). This results in a constant slope on the CO_2 concentration over time (when plotted with half-logarithmic scales).

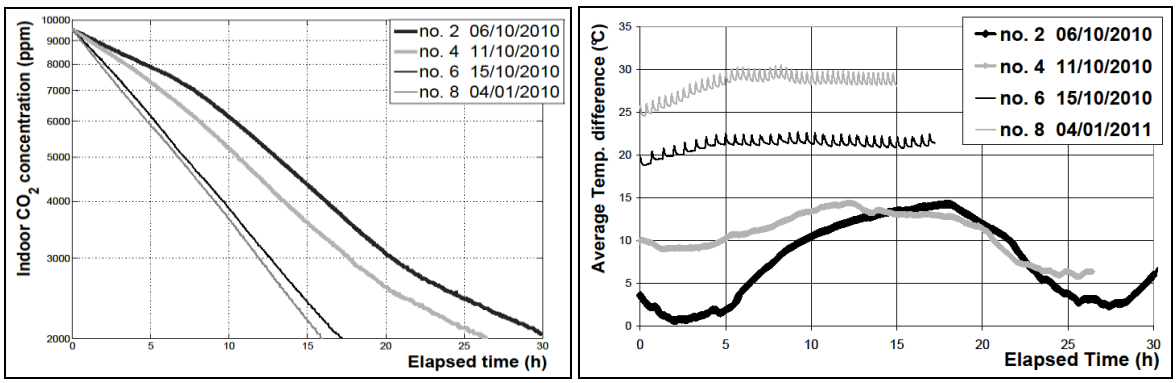

Fig. 5: Indoor concentration decay for a few experiments with half-logarithmic scales (a) and temperature difference (b) occurring during experiments no. 2, 4, 6 and 8.

The highest average wind speed value was recorded during experiment no. 10, which corresponds to the highest measured airflow rate. However, since wind speed did not remain constant during a single experiment, but indeed could vary substantially, more information was obtained by subdividing some experimental runs into short period. Experiment no. 1 was split in two parts to resolve one period lasting 3 hours where the mean wind speed was recorded at 6.6 $m.s^{-1}$ and a longer second period during which the wind speed had decreased to 1.2 $m.s^{-1}$ (see Fig. 6(b)). This resulted in a significantly slower decrease rate of the indoor concentration as presented in Fig. 6(a).

The air change rate for experiment no. 10 was observed to be greater than for experiment no. 1a, despite comparable and high wind speeds for both periods. The main difference was noted to be wind direction: for no. 1a the wind blew mainly towards the east whereas for no. 10 it blew towards the west.

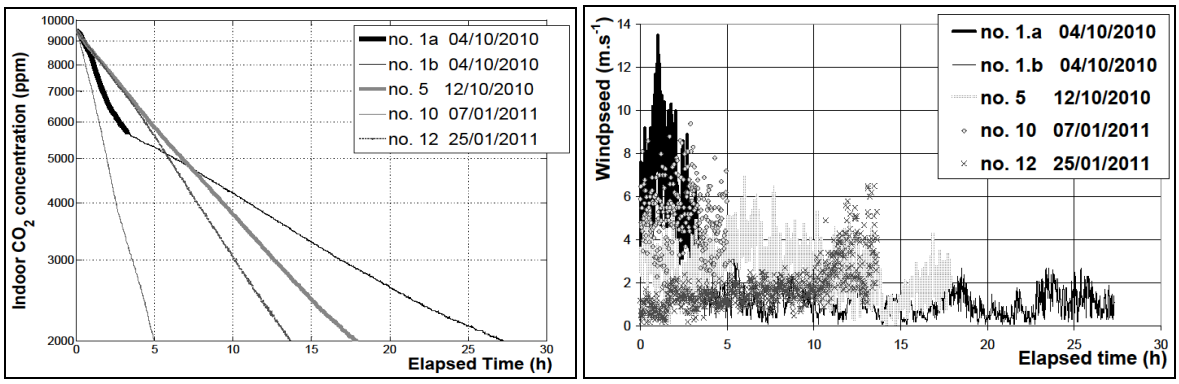

Fig. 6: Indoor concentration decay for a few experiments with half-logarithmic scales (a) and wind speed at 10 m (b) occurring during experiments no. 1, 5, 10 and 12.

From a general point of view, it is very convenient to consider average weather conditions and the total elapsed time to give a quick overlook of the experimental conditions and results. To explain the air change rate variations observed however, one should consider weather conditions in great detail. In the following sections, instantaneous weather conditions will be used to model air flows.

5.2 Air transfer model

Equations presented in part 4 were implemented in a Matlab / Simulink environment and a variable time-step solver was used to solve the mass balance at the building scale. Because of the uncertainties related to wind and thermal effects, the model was tested repeatedly with different values for h_{Wall}, h_{Door} and {k; a}. In order to compare each solution, computed air change rates were used to recalculate the tracer gas decrease and computed elapsed times were set against measurements. Somehow, this represents the model's mean accuracy.

A more detailed approach was used to complement the average performance. Indeed, in some cases comparisons based only on the elapsed time are not relevant. For example, an important error occurring at a single time step may result in a permanent bias on the elapsed time, as illustrated in Fig. 7(a). Equation (2) was changed to (10) to compute the hourly averaged air change rate from tracer gas measurements. The results are plotted in Fig. 7(b) as "Measurements".

$$Q_V = \frac{V}{\Delta t} \cdot \ln\left(\frac{C_{In}(t) - \overline{C_{Out}}}{C_{In}(t+\Delta t) - \overline{C_{Out}}} \right) \tag{10}$$

where Δt (h) is the time step, here equal to 1 h.

Preliminary simulations showed that the model was very sensitive to the equivalent door height h_{Door}, poorly sensitive to h_{Wall} and behaved differently from terrain coefficient values. This could be a consequence of the rather complex interaction between wind and thermal effects, as shown in Li *et al.* (2001). When considering both the elapsed time and the averaged error on the air change rate, the best solution used a "scattered" terrain coefficient; h_{Door} = 2 m; h_{Wall} = 0.75 m.

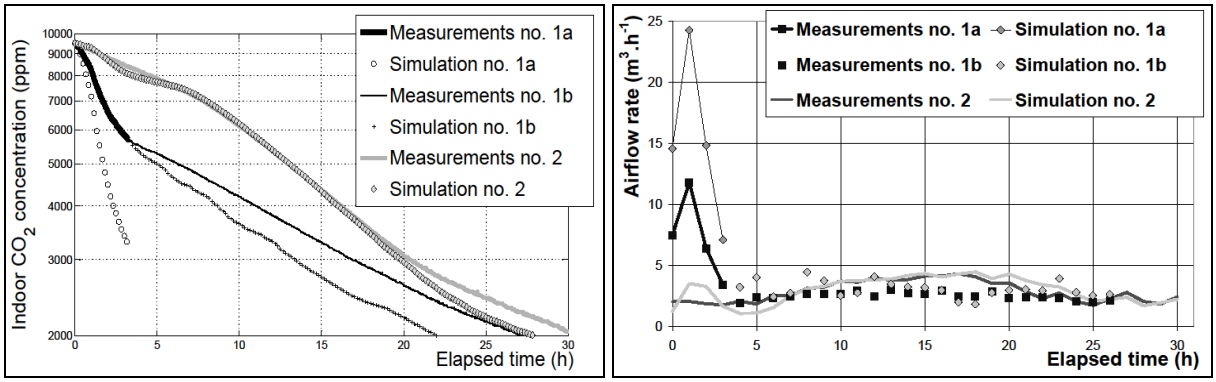

Fig. 7: Comparison of measured tracer gas decay (a) and airflow rate (b) ("scattered" terrain coefficient; h_{Door} = 0.01 m; h_{Wall} = 0.75 m) for experiments no. 1 and no. 2.

Detailed errors are presented in Table 7 for the best coefficient combination. A negative error on elapsed time means that the model overestimates the airflow rate.

Table 7: Error computed on the time duration and the air flow rate for each experimental sequence with the best parameter combination

N°	1.a	1.b	2	3	4	5	6	7	8	9	10	11	12
Measured Qv ($m^3.h^{-1}$)	8.4	2.6	3.0	3.4	3.4	5.0	5.2	6.0	5.6	4.6	18.0	4.7	6.6
Error Elapsed time	−54 %	−22 %	−14 %	−7 %	−18 %	−7 %	1 %	2 %	8 %	−31 %	3 %	5 %	1 %

Absolute error Q_V	82 %	27 %	24 %	11 %	24 %	14 %	12 %	25 %	19 %	47 %	15 %	20 %	18 %

The average error on elapsed time is 15 %, 23 % when looking at the air change rate. Experiment no. 7 shows the necessity of studying errors on both the elapsed time and the airflow rates: the computed airflow rates are 25 % accurate and can be either overestimated or underestimated. The errors at different time steps compensate each other, so that the computed elapsed time almost matches the measured value.

Still, these results are not homogeneous, meaning that the model has possibly encountered limits. Indeed, the airflow rate error exceeds 2.2 $m^3.h^{-1}$ for experiment no. 9 and may have been overestimated by 82 % for experiment no. 1.a when the measured airflow rate was 8.4 $m^3.h^{-1}$.

When looking at weather conditions, it becomes apparent that the wind speed V_{10} is greater than 5 $m.s^{-1}$ when the highest errors are computed. However, computed airflow rates were correctly estimated for experiment no. 10, which also occurred under high wind speed. This could be a consequence of the use of C_P values (see Table 4) to model the influence of wind incidence: this is consistent with earlier observations (see 4.1). In order to illustrate this statement, C_P values from (Hagentoft 2001) were used to replace the previous values. Both references are compared in Fig. 8 and the elapsed times are presented in Table 8.

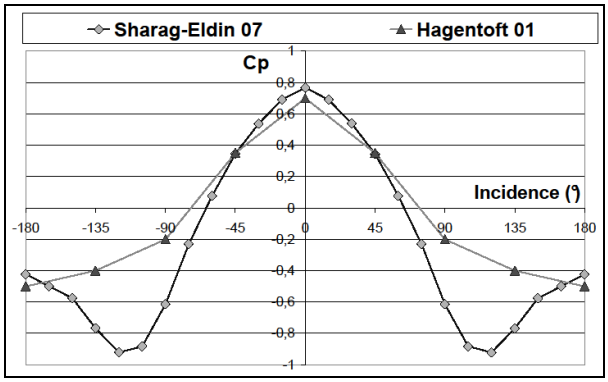

Fig. 8: Comparison of C_P values according to (Sharag-Eldin 2007) and (Hagentoft 2001)

Table 8: Error on the elapsed time using C_P values according to (Sharag-Eldin 2007) and to (Hagentoft 2001)

N°	1.a	1.b	2	3	4	5	6	7	8	9	10	11	12
Measured Qv ($m^3.h^{-1}$)	8.4	2.6	3.0	3.4	3.4	5.0	5.2	6.0	5.6	4.6	18.0	4.7	6.6
Sharag-Eldin 2007	82 %	27 %	24 %	11 %	24 %	14 %	12 %	25 %	19 %	47 %	15 %	20 %	18 %
Hagentoft 2001	63 %	12 %	19 %	32 %	26 %	19 %	6 %	26 %	16 %	99 %	25 %	15 %	16 %

The influence of C_P values is not homogeneous, which attests to how sensitive the model is. However, the trend is not very clear: better results can be achieved using (Hagentoft 2001) C_P values (experiments no. 1.a, 1.b, 6, 11) as well as less accurate results (experiments no. 3, 9, 10). Moreover, the influence can be sizeable with lower wind speed conditions if the thermal effect is less dominating (experiments no. 3 and no. 6). With high wind speed conditions, even if an improvement is observed for experiment no. 1, the results are less accurate for experiments no. 9 and no. 10. From a general point of view, better results were obtained with C_P values coming from (Sharag-Eldin 2007).

5.3 Outlook

Depending on the desired level of accuracy, one could investigate the numerical fitting further by setting C_P values in great detail. This could be achieved by studying the air flow around the tested building, which seems to be reasonable with respect to recent numerical improvements as presented in Obrecht *et al.* (2011).

In this case however, the air transfer model developed will be implemented in a more global model called HAM-Tools (Kalagasidis *et al.* 2007) to study the interactions between heat, air and moisture transfers. Weather data was analysed over a 6-month period. This has revealed that 95 % of the measured V_{10} values are below the 5 $m.s^{-1}$ limit. This would indicate that the 12 experiments were carried out under a representative climate. The model is thought to be accurate enough to further investigate the coupling with such transfers, estimating the potential of natural ventilation to limit indoor vapour excess, for example. In the same vein, this approach could be extended to other pollutants.

Using tracer gas measurements has been found to be effective when fitting a general model, and its applicability to other buildings seems promising. However, a few limitations must be mentioned. Firstly, using tracer gas measurements with multizonal buildings needs to be validated further. Secondly, it is important to underline the importance of achieving tracer gas measurements under representative climates; another experimental campaign would need to be carried out if different average weather conditions were to be considered. So, the legitimate domain is the second limit of this approach.

6. Conclusions

The tracer gas method was used to obtain air change rate measurements in a 50 m^3 natural ventilated building. Twelve experiments were conducted from October to January under varying wind and thermal conditions, with the air change rate ranging from 3 to 18 $m^3.h^{-1}$. As these rates are rather low, the experiment time lasted from 5 to 30 h. This is long enough to ignore short-term weather variations and allow us to consider general weather and wind data.

A classical single-node pressure model was used to estimate the global air change rate. General correlations were used to represent both wind and thermal effects. Experimental results were used to fit numerically obtained wind and thermal coefficient values. The results are 15% accurate when considering the elapsed time and 23 % when considering the global air change rate. As the uncertainties are related to the use of general pressure coefficients from the literature, better results could probably be obtained using wind-tunnelling or CFD simulations. Still, this method should remain valuable because of its simplicity and cost.

7. Acknowledgements

The authors would like to thank ADEME (the French Environment and Energy Management Agency, OPTI-MOB project, n°0704C0099) for its financial support.

8. References

Afonso C., Oliveira A., 2000 Solar Chimneys: simulation and experiment, Energy and Buildings 32 71-79

Baker J.T., Kim S.H., Gitz D.C., Timlin D., Reddy V.R., 2004 A method for estimating carbon dioxide leakage rates in controlled-environment chamber using nitrous oxide, Environmental and Experimental Botany 51 103-110

Blondel A., Plaisance H., 2011, Screening of formaldehyde indoor sources and quantification of their emission using a passive sampler, Building and Environment 46 1284-1291

Chao C.Y., Wan M.P., Law A.K., 2004, Ventilation performance measurement using constant concentration dosing strategy, Building and Environment 1277-1288

Cheong K.W., 2001, Airflow measurements for balancing of air distribution system – tracer gas technique as an alternative? Building and Environment 36 955-964

Collignan B., O'Kelly P., Ribéron J., 2005, Use of metabolic-related carbon dioxide as tracer gas for assessing air renewal in dwellings, Indoor Air 2005 conference, September 4-9, Beijing, China

Costola D., Blocken B., Ohba M., Hensen J.L.M., 2010, Uncertainty in airflow rate calculations due to the use of surface-averaged pressure coefficients, Energy and Buildings 42, p.881–888

Janssens A., Hens H., 2007, Effects of wind on the transmission heat loss in duo-pitched insulated roofs: a field study, Energy and Building 39 1047-1054

Kalagasidis A.S., Weitzmann P., Nielsen T.R., Peuhkuri R., Hagentoft C.E., Rode C., 2007, The international building physics toolbox in Simulink, Energy and Building, 39 665-674

Karlsson J.F., Moshfegh B., 2007, A comprehensive investigation of a low energy building in Sweden, Renewable Energy, 32 1830-1841

Koinakis C.J., 2005, The effect of the use of openings on interzonal air flows in buildings: an experimental and simulation approach, Energy and Building, 37 813-823

Koffi J., 2009, Analyse multicritère des stratégies de ventilation en maisons individuelles, Doctoral Thesis, Université de La Rochelle, France

Hagentoft C.E., 2001 Introduction to Building Physics, Studentlitteratur, Lund, Sweden ISBN 91-44-01896-7

Laporte S., Virgone J., Castanet S., 2001, A comparative study of two tracer gases : SF6 and N2O, Building and Environment 36 313-320

Larsen T.S., Heiselberg P., 2008, Single-sided natural ventilation driven by wind pressure and temperature difference, Energy and Buildings 40 1031-1040

Li Y., Delsante A., Chen Z., Sandberg M., Andersen A., Bjerre M., Heiselberg P., 2001, Some examples of solution multiplicity in natural ventilation, Building and Environment 36 851-858

Obrecht C., Kuznik F., Tourncheau B., Roux J.J., 2011, Towards urban scale flow simulations using the Lattice Boltzmann method, Proceedings of Building Simulation, 12th Conference of International Building Performance Simulation Association, Sydney, 14-16 November

Piot A, Woloszyn M, Brau J, Abele C., 2011, Experimental wooden frame house for the validation of whole building heat and moisture transfer numerical models, Energy and Buildings 43, 1322-1328

Piot A., 2009, Hygrothermique du bâtiment : expérimentation sur une maison à ossature bois en conditions climatiques naturelles et modélisation numérique, PhD thesis, INSA-Lyon, France

Santamouris M., Synnefa A., Asssimakopoulos M., Livada I., Pavlou K., Papaglastra M., Gaitani N., Kolokotsa D., Assimakopoulos V., 2008, Experimental investigation of the air flow and indoor carbon dioxide concentration in classrooms with intermittent natural ventilation, Energy and Building 40 1833-1843

Sfakianaki A., Pavlou K., Santamouris M., Livada I., Assimakopoulos M.N., Mantas P., Christakopoulos A., 2008, Air tightness measurements of residential houses in Athens, Greece, Building and Environment 43 398-405

Sharag-Eldin A., 2007, A parametric model for predicting wind-induced pressures on low-rise vertical surfaces in shielded environments. Solar energy 81, 52–61

Tanner D.J., Cleland A.C., Robertson T.R., Opara L.U., 2000, Use of carbon dioxide as a tracer gas for determining in package airflow distribution, Journal of Agricultural Engineering Research 77 409-417

Uematsu Y., Isyumov N., 1999, Wind pressure acting on low rise buildings, Journal of Wind Engineering and Industrial Aerodynamics 82 1-25

Van Buggenhout S., Van Brecht A., Ozcan S.E., Vranken E., Van Malcot W., Berckmans D., 2009, Influence of sampling positions on accuracy of tracer gas measurements in ventilated spaces, Biosystems Engineering 104 216-223

Van Hoof T., Blocken B., 2010, On the effect of wind direction and urban surroundings on natural ventilation of a large semi-enclosed stadium, Computers & Fluids 39 1146–1155

Walker I.S., Wilson, D.J., Sherman M.H., 1998, A comparison of the power law to quadratic formulations for air infiltration calculations, Energy and Buildings 27 293-299

Woloszyn M., Kalamees T., Abadie M.O., Steeman M., Kalagasidis A.S., 2009, The effect of combining a relative-humidity-sensitive ventilation system with the moisture buffering capacity of materials on indoor climate and energy efficiency of buildings, Building and Environment 44 515-524